



ELSEVIER

Nuclear Physics A 693 (2001) 517–532



www.elsevier.com/locate/npe

Lifetimes in the middle of $1f_{7/2}$ shell: cross-conjugated nuclei ^{47}V and ^{49}Cr

F. Brandolini^{a,*}, N.H. Medina^b, S.M. Lenzi^a, D.R. Napoli^c, A. Poves^d,
R.V. Ribas^b, J. Sanchez-Solano^d, C.A. Ur^a, M. De Poli^c, N. Mărginean^c,
D. Bazzacco^a, J.A. Cameron^e, G. de Angelis^c, A. Gadea^c,
R. Menegazzo^a, C. Rossi-Alvarez^a

^a Dipartimento di Fisica dell' Università and INFN, Sezione di Padova, Padova, Italy

^b Instituto de Física, Universidade de São Paulo, São Paulo, Brazil

^c Laboratori Nazionali di Legnaro – INFN, Legnaro, Italy

^d Departamento de Física Teórica, Universidad Autónoma, Cantoblanco, Madrid, Spain

^e Department of Physics and Astronomy, McMaster University, Hamilton, Canada

Received 27 December 2000; revised 5 February 2001; accepted 13 February 2001

Abstract

DSAM lifetimes have been determined in the middle of $1f_{7/2}$ shell for the cross-conjugated nuclei ^{47}V and ^{49}Cr , populated with the reaction ^{28}Si on ^{28}Si at 115 MeV using a Au backed target. $B(E2)$ and $B(M1)$ reduced rates agree very well with large scale shell model predictions. The interplay between spherical and collective structures is discussed. © 2001 Elsevier Science B.V. All rights reserved.

PACS: 21.10.Tg; 23.20.-g; 23.20.Lv; 27.40.+z

Keywords: NUCLEAR REACTION $^{28}\text{Si}(^{28}\text{Si},2\alpha p)$, $^{28}\text{Si}(^{28}\text{Si},\alpha 2pn)$, $E = 115$ MeV; Measured E_γ , I_γ , $\gamma\gamma$ -coincidence, DSA; ^{47}V and ^{49}Cr deduced high-spin levels, J , π , τ , $B(E2)$, $B(M1)$

1. Introduction

In recent years extensive and detailed experimental studies were performed in the $1f_{7/2}$ shell using the GASP multidetector array [1–4]. The new data turned out to be generally in good agreement with Large Scale Shell Model (LSSM) calculations made by the Strasbourg–Madrid collaboration [5–9]. That group has given an important contribution to clarify the connection between LSSM and collective rotations, also with the development of the quasi- $SU(3)$ model [8,10]. The possibility to directly interpret the

* Corresponding author.

E-mail address: brandolini@pd.infn.it (F. Brandolini).

LSSM calculations, not only looking for single-particle properties, but also for typical collective phenomena, has greatly increased the interest for this approach, contradicting the rather diffuse opinion that Shell Model (SM) calculations may not reveal the underlying collective structure. In this context the nuclei in the middle of the $1f_{7/2}$ shell turned to be a unique workbench where most of the concepts related to collective properties such as axial and triaxial deformation, band crossing, band termination, particle–rotor coupling, etc., find their microscopical explanation in the spherical SM framework. An essential role in this comparison is played by electromagnetic moments and, in this context, by Doppler shift attenuation method (DSAM) lifetime measurements. One should underline that $B(M1)$ reduced rates are specifically sensitive to single particle features, while $B(E2)$ values to rotational collectivity. Good agreement was found for $B(E2)$ and $B(M1)$ reduced rates in the ground-state bands in even–even nuclei ^{48}Cr and ^{50}Cr [3].

This paper is principally aimed to provide precise experimental $B(E2)$ and $B(M1)$ reduced rates for the ground-state bands in the nuclei ^{47}V and ^{49}Cr . Some extensions of the level schemes will be also presented. It has to be recalled that ^{47}V and ^{49}Cr are cross-conjugated nuclei in the $1f_{7/2}$ shell, and that their level schemes should be identical in that configuration space. Since this is not the case, as can be seen in Figs. 1 and 2, standard calculations in the $1f_{7/2}$ shell [11,12] are not adequate and SM calculations in a larger configuration space are required. LSSM calculations in the full fp configuration have been already reported in Ref. [8], where the rotational properties are discussed in detail. An experiment was recently performed in quite similar experimental conditions but a detailed comparison with SM predictions was not possible because of the rather poor statistics [13].

New experimental information is also reported here for the unnatural parity band with $K^\pi = 3/2^+$ in ^{47}V , which has been described as a $1d_{3/2}$ proton–hole coupled to the ^{48}Cr ground-state (gs) band [9]. Unnatural parity states in ^{49}Cr have been already described by us in a recent publication [4]. In this case two bands, with $K = 3/2^+$ and $13/2^+$, are originated by the coupling of a $1d_{3/2}$ proton–hole with the low lying $K = 0^+$, $T = 1$ and the $K = 5^+$, $T = 0$ bands in ^{50}Mn , respectively. Part of the present data has been recently presented at a conference [14].

2. Experimental procedure

High-spin states have been populated in the reaction ^{28}Si on ^{28}Si at 115 MeV bombarding energy. The beam was provided by the Tandem XTU accelerator of the Legnaro National Laboratories and the target consisted of 0.8 mg/cm^2 of ^{28}Si on 15 mg/cm^2 of Au. The mean initial velocity of the recoils was $0.045 c$. The nuclei ^{47}V and ^{49}Cr were populated by the $(2\alpha p)$ and $(\alpha 2pn)$ evaporation channels, respectively. Coincident γ -rays were collected with the γ -spectrometer GASP, which consists of 40 Compton-suppressed large volume detectors and a BGO multiplicity filter with 80 elements. Events were stored when at least two Ge detectors and two elements of the multiplicity filter fired in coincidence. The data were sorted into 7 γ - γ matrices having on the first axis the detectors at average angles 34° , 60° , 72° , 90° , 108° , 120° , and

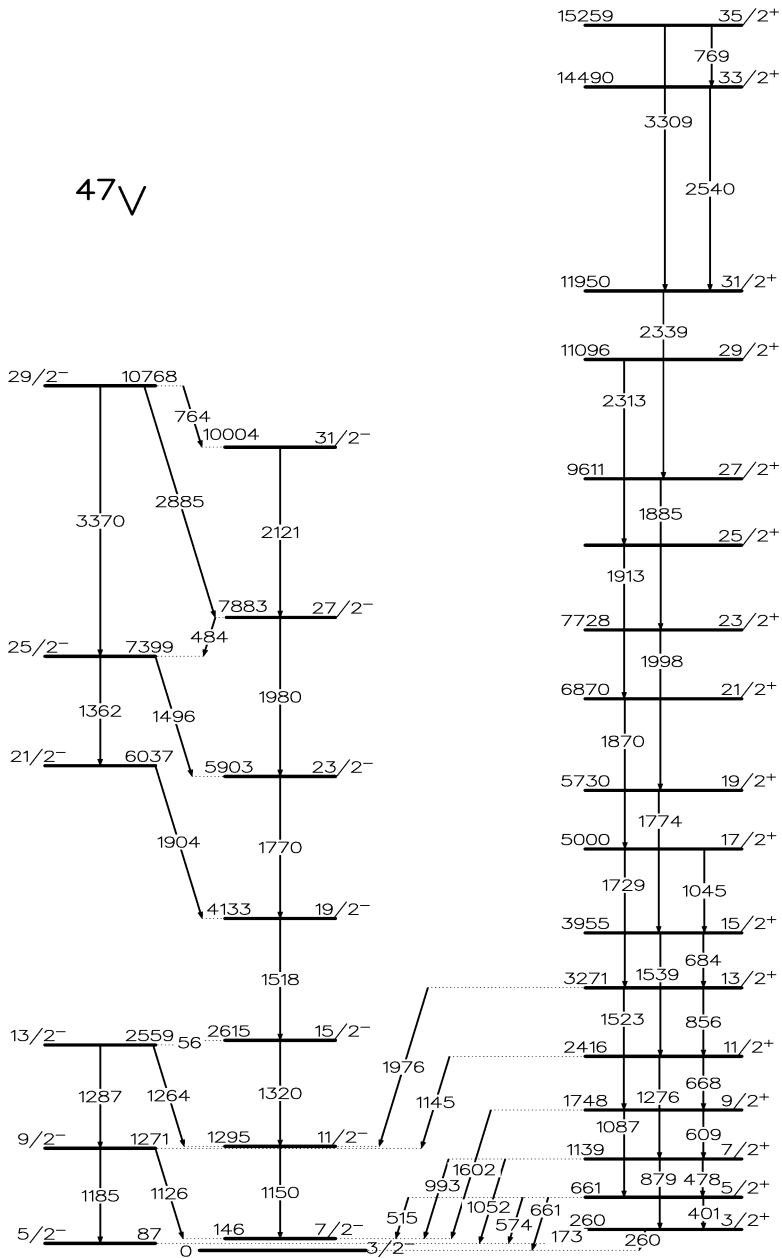


Fig. 1. Adopted level scheme(s) of ^{47}V .

146°, respectively, and on the second axis all the other detectors. Energy and intensity calibrations were performed with sources of ^{152}Eu and ^{56}Co , as well as with internal narrow lines. The intrinsic lineshape was evaluated by inspecting several narrow lines present in the coincidence spectra. Further experimental details can be found in Ref. [3].

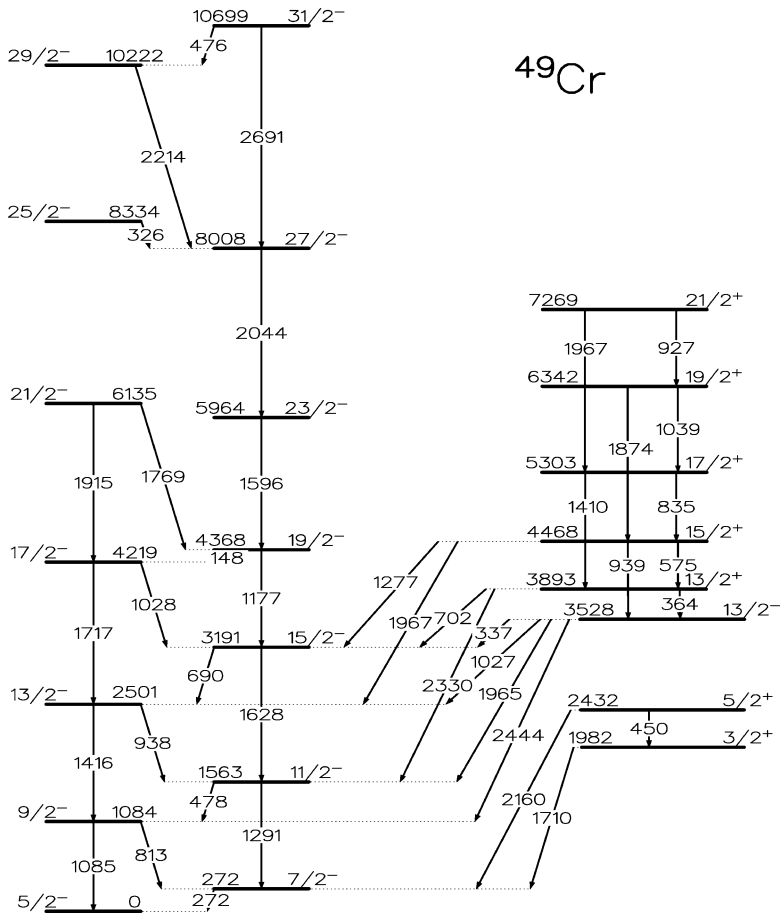


Fig. 2. Adopted level scheme(s) of ^{49}Cr .

Lifetimes have been determined both with the standard DSAM procedure and with the Narrow Gate on Transitions Below (NGTB) procedure [15], which is free from systematic errors related with the sidefeeding and was successfully employed in previous works [3,4, 16]. In brief, this method consists of setting a gate on the unshifted part of the lineshape of a broadened transition. This results in a suppression of the shifted component of the lineshape for a transition above it, taken as a probe, which depends only on the lifetime associated to the gating transition. The DSAM analysis was performed with the program LINESHAPE [17], modified to include also the NGTB procedure.

The DSAM analysis proceeded as follows. In a first phase a standard DSAM analysis has been performed, accounting for the sidefeeding population determined experimentally. After this step several lifetime assignments were rather poor, owing to the feeding time uncertainty. In a second phase, the NGTB procedure has been applied, using the previous fit for the probe lineshape. The γ -ray lineshapes were taken as probe when they showed a relevant broadening, but accompanied by some unshifted component.

As in previous papers based on the same experimental data [3,4], the Northcliffe–Schilling (NS) electronic stopping power [18], corrected for atomic shell effects [23], was used in combination with the LSS term for the nuclear stopping [19]. It has to be noted that in DSAM lifetime analysis some other parameterizations for the electronic part have been adopted, among them the most used is the Ziegler, Biersack, Littmark one [20]. It has been shown in Ref. [21], however, that, in spite of being more recent, it may be not the best to be used in DSAM analysis because the extrapolation to low velocities can be poor. This is not the case of the NS one which guarantees a smooth matching with a linear dependence on the velocity at low energy, which is theoretically predicted and experimentally confirmed [22]. In the present case several data for stopping in Au of ions close of those of interest are implemented in the parameterization, with the consequence the Ziegler, Biersack, Littmark and NS parameterizations are nearly identical at high velocities while they differ at most by 10% at $v/c = 0.02$, where the NS one is lower. On this basis the systematic error on the lifetimes due to the stopping power was taken as 8% for rather fast transitions, when associated to a well shifted lineshape, while was increased up to 15% for the others. The quality of the stopping power down to low velocities was probed by checking the rather precise lifetimes of 1.43(13) and 2.34(14) ps of the 4^+ and 6^+ levels in ^{46}Ti [24]. When analyzing with the standard procedure lineshapes with a small shifted component, a further contribution to the systematic error was due to the gaussian description of the intrinsic lineshape.

In the case of the NGTB procedure for short lifetimes, which also results in lineshapes with a small tail, another systematic error may arise from the fact that two separate average velocity distributions are assumed for the two coincident γ -ray lines. In order to check a possible effect due to some correlation between the decays of the two coincident γ -rays during the same slowing down process, simulated γ -spectra, obtained accounting correctly for the correlation, were analysed with NGTB. In this way the systematic error was estimated to be less than 5% down to lifetime values of 0.1 ps.

In the following only examples of NGTB analysis will be reported but the best fit obtained for probe transitions provides an estimate of the quality for data obtained with the standard procedure, which allowed the determination of several lifetimes. The reported lifetime determinations are usually the average of the analysis at different angles, eventually with the exclusion of some comparatively more contaminated spectra. Disagreement was found in some cases with previous values reported in Ref. [13].

3. Experimental results

3.1. The nucleus ^{47}V

The level scheme of the nucleus ^{47}V , reported in Fig. 1, agrees with that of Ref. [13] with the important variation that the 1904–1362 keV sequence is now put in reversed order. This was already noticed in Refs. [9,25]. Only yrast levels of both parities are reported. Some observed transitions, that could not be univocally located are not displayed: this is the case

of the 2874, 831 and 261 keV lines which seem to entry in the level scheme at the $23/2^-$ level. A peculiar fact is that the yrast $17/2^-$ state, theoretically predicted close to the $19/2^-$ one, has not been observed. Some data for the $9/2^-$ and $13/2^-$ levels were taken from Ref. [26], as they were only weakly populated in our reaction. A weak 56 keV branching connecting the $15/2^-$ to the $13/2^-$ level could be established indirectly, by estimating the relative intensity of the 1320 keV and 1264 keV lines in coincidence with the 1518 keV line. The decay of the $29/2^-$ level at 10768 keV is found to proceed via three branchings. The 2874 keV line made troublesome the determination of the 2885 keV branching, which in Ref. [13] was apparently overestimated due to its contamination.

The positive parity band, reported in Ref. [13], is now extended up to the terminating state $35/2^+$. A 1931 keV line populating the $11/2^+$ state was not plotted.

Several new lifetimes have been determined. Examples of γ -ray lineshape analysis are reported in Fig. 3. A NGTB analysis is shown in the upper part of Fig. 3 for the determination of the lifetime associated to the 1980 keV ($27/2^- \rightarrow 23/2^-$) transition, using the 2121 keV ($31/2^- \rightarrow 27/2^-$) transition as probe. The large suppression indicates a short lifetime as compared with the stopping time. A NGTB analysis is reported in the lower part of Fig. 3 for determining the lifetime value of 0.25(4) ps for the $13/2^+$ state, gating on the 1523 keV ($13/2^+ \rightarrow 9/2^+$) transition and using the 1728 keV ($17/2^+ \rightarrow 13/2^+$) transition as probe. For this state a lower limit of 3 ps was previously reported in Ref. [13].

The experimental data are shown in Table 1, where previous data were taken from Ref. [26] and the more recent Ref. [13]. It is specified for which transition also a NGTB analysis has been performed. Consistent data were generally obtained with the two procedures and NGTB values are reported, when available. The experimental $B(E2)$ and $B(M1)$ reduced rates, obtained in the present experiment, are shown in Fig. 4, for an easier comparison with theory. For reason of completeness, previous data referring to levels not studied in the present work, are also reported. $B(E2)$ rates have been determined only for stretched transitions. Mixing ratios are known for some lower transitions with $\Delta I = 1$ [26]. The absolute values $|\delta|$ of the mixing ratios are in general small with the exception of the 1126 keV ($9/2^- \rightarrow 7/2^-$) transition for which $\delta = -0.43(6)$ is reported, which leads to a $B(E2)$ value two times larger than predictions. The other values are generally consistent with zero, but for the 87 keV ($5/2^- \rightarrow 3/2^-$) transition $\delta = 0.125(21)$ is given, corresponding to 240(80) W.u., which is not realistic. For higher transitions δ is not known, but is predicted to be small enough so that its contribution is estimated to be within the quoted $B(M1)$ error bars. For the lower levels, the E1 branching ratios of Ref. [26] were adopted. The transitions in Fig. 4 are identified by the higher spin connected by them. Only a lower limit was obtained for the $B(M1)$ value of the $29/2^- \rightarrow 27/2^-$ transition and the $B(E2)$ of the $29/2^- \rightarrow 25/2^-$ transition. We note however that the $29/2^- \rightarrow 31/2^-$ transition is about 30 times favored with respect to the $29/2^- \rightarrow 27/2^-$ one. We can thus obtain an upper limit for the latter, adopting a reasonable upper limit for the former. Experimentally, only few $B(M1)$ rates in the $1f_{7/2}$ shell are as large as about one μ_N^2 . On the basis of shell model calculations in the $1f_{7/2}^n$ space [12] one can reasonably estimate an upper limit of $3.2 \mu_N^2$ for the $B(M1)$ value of this transition in ^{47}V . Adopting in the present case $4 \mu_N^2$, the $B(M1)$ value for the $29/2^- \rightarrow 27/2^-$ transition is derived to be smaller

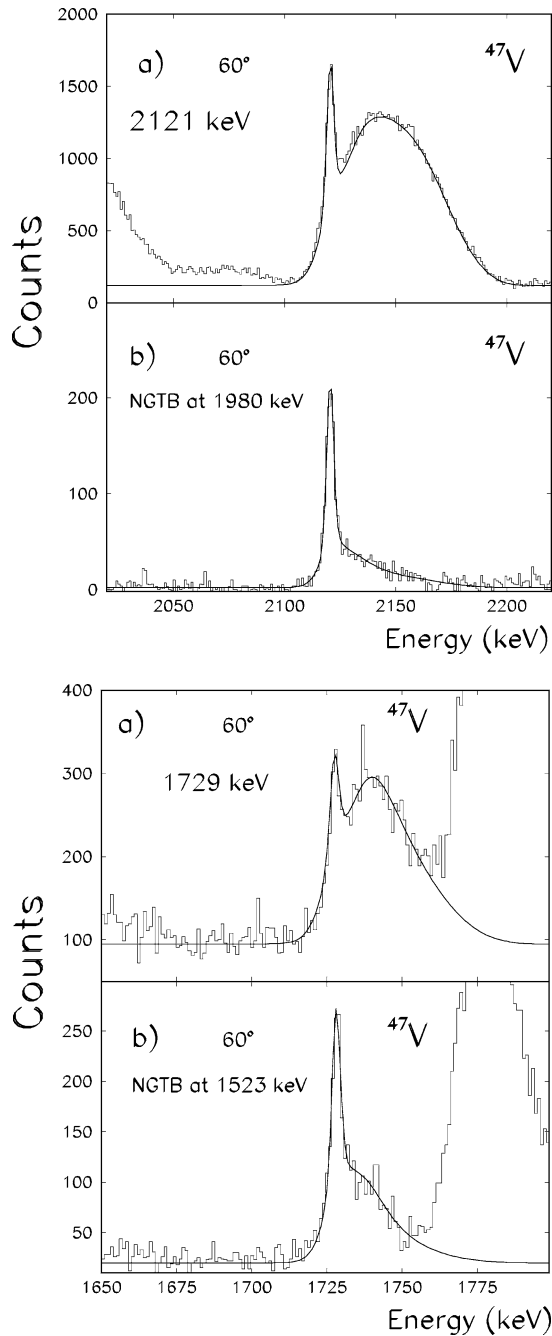


Fig. 3. DSAM lineshape analysis in ^{47}V : (upper part) NGTB analysis for the $27/2^-$ state gating on the $1980\text{ keV } 27/2^- \rightarrow 23/2^-$ transition and using as probe the 2121 keV transition; (lower part) NGTB analysis for the $13/2^+$ state, gating on the $1523\text{ keV } 13/2^+ \rightarrow 9/2^+$ transition and using the $1729\text{ keV } 17/2^+ \rightarrow 13/2^+$ transition as probe.

Table 1
Experimental results in ^{47}V

Transition	E_γ exp. keV	E_γ SM keV	γ -Int	γ -BR exp. %	τ exp. ps	τ prev. ps	$B(E2)$ exp. $e^2 \text{ fm}^4$	$B(E2)$ th. $e^2 \text{ fm}^4$	$B(M1)$ exp. μ_N^2	$B(M1)$ th. μ_N^2
$5/2^- \rightarrow 3/2^-$	87.5	49	52	100		961(60) ^a	2418(800)	251	0.082(5)	0.12
$7/2^- \rightarrow 3/2^-$	145.8	104	0.5	1.0(3)		721(85) ^a	170(70)	106		
$7/2^- \rightarrow 5/2^-$	58.2	55	50	99.0(3)				201	0.35(4)	0.24
$9/2^- \rightarrow 5/2^-$	1184.5	1262	0.2	18(2) ^a		0.35(11) ^a	180(60)	138		
$9/2^- \rightarrow 7/2^-$	1125.7	1207	1.0	82(2) ^a			158(60)	75	0.09(3)	0.08
$11/2^- \rightarrow 7/2^-$	1149.5	1163	100	100	2.5(8) ^c	2(1) ^a	162(52)	186		
$13/2^- \rightarrow 9/2^-$	1287.0	1182	0.8	38(4) ^a			146(51)	158		
$13/2^- \rightarrow 11/2^-$	1263.8	1226	1.1	62(4) ^a	0.6(2)			30	0.029(10)	0.043
$15/2^- \rightarrow 11/2^-$	1320.0	1278	93	99.8(6)	0.99(10) ^c	$< 2^a, > 2.5^b$	205(25)	187		
$15/2^- \rightarrow 13/2^-$	(56.2)	52	0.2	20(6)				55	0.68(23)	0.70
$19/2^- \rightarrow 15/2^-$	1517.8	1522	90	100	0.60(6) ^c	0.70(10) ^b	169(17)	130		
$21/2^- \rightarrow 19/2^-$	1903.7	2067	8.1	100	< 0.20			3.3	> 0.04	0.13
$23/2^- \rightarrow 19/2^-$	1769.8	1907	73	100(5)	0.35(3) ^c	0.50(7) ^b	134(13)	135		
$25/2^- \rightarrow 21/2^-$	1362.1	1527	4.1	8(2)			107(31)	102		
$25/2^- \rightarrow 23/2^-$	1495.9	1732	45	92(2)	0.13(2) ^c	0.34(5) ^b		5.4	0.120(19)	0.15
$27/2^- \rightarrow 23/2^-$	1980.4	2187	21.7	35(5)	0.16(2) ^c	0.14(3) ^b	58(11)	98		
$27/2^- \rightarrow 25/2^-$	484.4	455	31.9	65(5)	"			6.6	2.0(3)	2.05
$31/2^- \rightarrow 27/2^-$	2121.0	2410	23.2	100(5)	0.37(3)	0.34(4) ^b	51(4)	54		
$29/2^- \rightarrow 31/2^-$	764.0	684	1.9	50(7)	< 0.08	< 0.14		6.1	> 1	3.25
$29/2^- \rightarrow 25/2^-$	3370	3559	1.2	30(5)			$9 < x < 45$	34		
$29/2^- \rightarrow 27/2^-$	2885	3103	0.7	20(6)				0.7	0.01 $< x < 0.14$	0.047

Errors in γ -ray energies are 0.4 keV rising to 1 keV above 2 MeV. Gamma-ray lines in brackets were not observed.

^aRef. [20].

^bRef. [12].

^cAlso with NGTB.

Table 1—continued

Transition	E_γ exp. keV	E_γ SM keV	γ -Int	γ -BR exp. %	τ exp. ps	τ prev. ps	$B(E2)$ exp. $e^2 \text{ fm}^4$	$B(E2)$ th. $e^2 \text{ fm}^4$	$B(M1)$ exp. μ_N^2	$B(M1)$ th. μ_N^2
$5/2^+ \rightarrow 3/2^+$	400.8	553	7.1	29.9(2)	> 4	2.3(17) ^a		463	< 0.067	0.015
$7/2^+ \rightarrow 3/2^+$	878.9	1023	9	32.5(4)	2.3(5) ^c	1.7(7) ^a	220(48)	207		
$7/2^+ \rightarrow 5/2^+$	478.2	471	7.2	25.0(4)	"	"		324	0.057(11)	0.023
$9/2^+ \rightarrow 5/2^+$	1086.8	1123	9	46(1)	0.80(12) ^c	0.88(12) ^a	309(47)	284		
$9/2^+ \rightarrow 7/2^+$	608.8	653	2.3	17(1)				181	0.054(9)	0.024
$11/2^+ \rightarrow 7/2^+$	1276.2	1398	26	86(1)	0.56(6) ^c	1.4(6) ^b	370(40)	350		
$11/2^+ \rightarrow 9/2^+$	667.8	746	3.2	11(1)				162	0.038(5)	0.029
$13/2^+ \rightarrow 9/2^+$	1522.5	1691	22	79(2)	0.25(4) ^c	> 3 ^b	315(51)	340		
$13/2^+ \rightarrow 11/2^+$	855.5	945	4.2	15(2)				79	0.055(11)	0.025
$15/2^+ \rightarrow 11/2^+$	1539.4	1760	28	92(2)	0.24(4) ^c	0.54(9) ^b	362(61)	369		
$15/2^+ \rightarrow 13/2^+$	684.0	815	2.4	8(2)				96	0.059(18)	0.031
$17/2^+ \rightarrow 13/2^+$	1728.6	1869	10	90(2)	0.15(5) ^c		317(106)	325		
$17/2^+ \rightarrow 15/2^+$	1045.2	1054	1.0	10(2)				40	0.033(13)	0.019
$19/2^+ \rightarrow 15/2^+$	1774.0	1971	24	100	0.115(25)	0.33(6) ^b	404(88)	329		
$21/2^+ \rightarrow 17/2^+$	1869.8	2111	8.1	100	< 0.30		> 120	224		
$23/2^+ \rightarrow 19/2^+$	1997.6	1921	15	100	0.10(3)	< 0.1 ^b	256(77)	206		
$25/2^+ \rightarrow 21/2^+$	1912.6	1970	3.2	100				138		
$27/2^+ \rightarrow 23/2^+$	1884.5	1671	9.3	100	0.20(8)	0.12(5) ^b	172(69)	148		
$29/2^+ \rightarrow 25/2^+$	2312.8	2508	2.4	100				108		
$31/2^+ \rightarrow 27/2^+$	2338.5	2398	6.0	100	0.12(2)	< 0.17 ^b	97(16)	117		
$33/2^+ \rightarrow 29/2^+$	(3394)	2919	–	< 10				51		
$33/2^+ \rightarrow 31/2^+$	2540.0	2600	1.5	> 90	< 0.1			0.3	> 0.03	0.051
$35/2^+ \rightarrow 31/2^+$	3309.0	3460	1.5	90(3)	< 0.1		> 20	61		
$35/2^+ \rightarrow 33/2^+$	769.1	860	0.2	10(3)				3.5	> 0.10	0.656

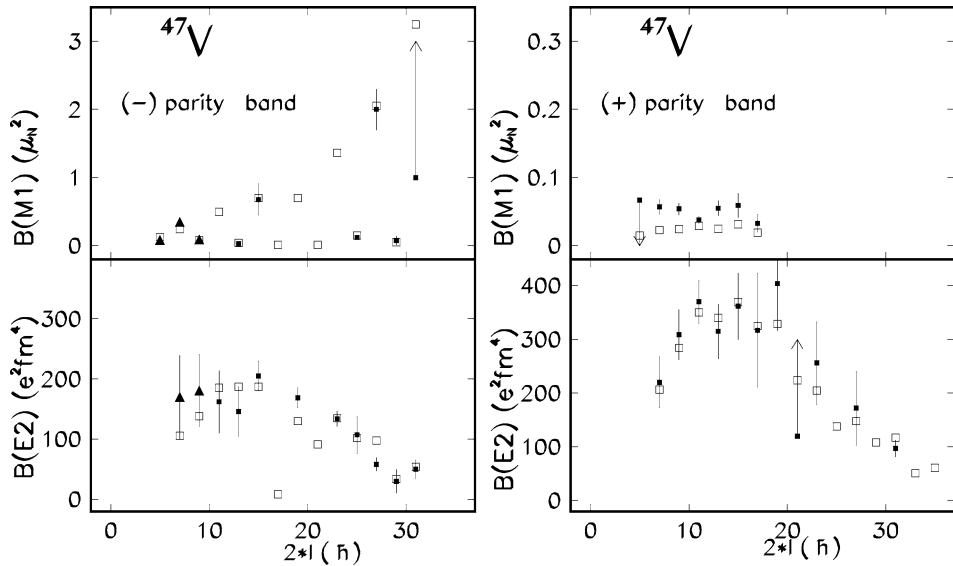


Fig. 4. Experimental $B(E2)$ and $B(M1)$ reduced transition rates in ^{47}V , compared with LSSM predictions (empty squares). Data are taken from the present work (full squares), except for those indicated as full triangles [20].

than $0.1 \mu_N^2$. Similarly, the $B(E2)$ value for the $29/2^- \rightarrow 25/2^-$ transition is estimated to be smaller than $50 e^2 \text{fm}^4$. The branching ratios of the $29/2^-$ level are predicted by LSSM to be 36, 26 and 38% for the transitions $29/2^- \rightarrow 31/2^-$, $29/2^- \rightarrow 27/2^-$, and $29/2^- \rightarrow 25/2^-$, respectively, to be compared with the experimental values 50(7), 20(6) and 30(5)%.

Finally, the two E1 transitions $13/2^+ \rightarrow 11/2^-$ of 1976 keV and $11/2^+ \rightarrow 9/2^-$ of 1145 keV resulted to have both a strength of about 2×10^{-5} W.u.

3.2. The nucleus ^{49}Cr

The level scheme of the nucleus ^{49}Cr is shown in Fig. 2. The ground-state band agrees with that of Ref. [13], while it has to be noted that in Ref. [27] the yrast $25/2^-$ level is located at 8879 keV, i.e. about 500 keV higher: it could be a yrare $25/2^-$ level. Coincidence γ - γ spectra gated on the 326 keV line, clearly indicate that this transition feeds directly the $27/2^-$ state. The very short lifetime observed is only consistent with M1 multipolarity since an E1 transition would be of 10^{-2} W.u., greatly exceeding the limit of 3×10^{-4} W.u. in this region [4]. The other possible branches of 2200 and 2370 keV were not observed, so that only a limit is given for them. It has to be noted that those γ -ray lines are expected to be very broad in our experimental conditions, making their observation difficult. Experimental data are summarized in Table 2. Previous data were taken from Ref. [28] or the more recent Ref. [13].

A couple of lineshape analysis examples are presented in Fig. 5. In the upper part of Fig. 5 it is shown that a large suppression of the 1177 keV line was obtained in the case

Table 2
Experimental results in ^{49}Cr

Transition	E_γ (keV)	E_γ (keV)	Int	BR (%)	τ (ps)	τ (ps)	$B(\text{E}2)$ ($e^2 \text{fm}^4$)		$B(\text{M}1)$ (μ_N^2)	
	exp.	SM					exp.	th.	exp.	th.
$7/2^- \rightarrow 5/2^-$	271.8	297	100	100		18(4) ^a	383(117)	322	0.16(4)	0.14
$9/2^- \rightarrow 5/2^-$	1084.9	1252	10	5(1)		0.22(4) ^a	122(27)	97		
$9/2^- \rightarrow 7/2^-$	812.6	955	56	95(1)			426(149)	283	0.46(9)	0.39
$11/2^- \rightarrow 7/2^-$	1290.8	1370	39	42(2)	0.57(6) ^c	0.53(9) ^a	168(25)	167		
$11/2^- \rightarrow 9/2^-$	478.4	415	46	58(2)			107(85)	215	0.53(5)	0.47
$13/2^- \rightarrow 9/2^-$	1416.4	1436	5.4	13(2)	0.15(2)	0.23(6) ^a	124(25)	191		
$13/2^- \rightarrow 11/2^-$	938.3	1021	53	87(2)				153	0.40(5)	0.63
$15/2^- \rightarrow 11/2^-$	1627.8	1620	20	31(2)	0.12(3) ^c	0.40(10) ^a	184(50)	188		
$15/2^- \rightarrow 13/2^-$	690.1	599	45.5	69(2)	"	"		96	1.0(3)	0.80
$17/2^- \rightarrow 13/2^-$	1717.4	1613	3.1	23(3)	0.09(3) ^{c,d}	0.22(3) ^b	140(36)	147		
$17/2^- \rightarrow 15/2^-$	1027.8	1188	10.5	77(3)	"	"		56	0.45(10)	0.30
$19/2^- \rightarrow 15/2^-$	1176.6	1256	55.5	95(1)	2.1(2) ^c	2.70(20) ^a	164(18)	156		
$19/2^- \rightarrow 17/2^-$	148.1	68	7.5	5(1)				69	0.44(10)	0.50
$21/2^- \rightarrow 17/2^-$	1915.0	2185	3.5	40(7)	0.10(3)	> 9 ^b	127(34)	116		
$21/2^- \rightarrow 19/2^-$	1768.9	2117	5.0	60(7)	"	"		37	0.062(14)	0.03
$23/2^- \rightarrow 19/2^-$	1596.3	1785	57.2	100	0.64(6) ^c	0.65(7) ^b	123(14)	142		
$27/2^- \rightarrow 23/2^-$	2043.8	2205	26	100	0.28(3) ^c	0.27(3) ^b	82(9)	86		
$25/2^- \rightarrow 27/2^-$	325.9	324	1.7	> 60	0.42(8)	< 0.43 ^b		13	> 1.9	1.77
$25/2^- \rightarrow 23/2^-$	(2370)	2530	< 0.6	< 20				0.4	< 0.002	0.001
$25/2^- \rightarrow 21/2^-$	(2199)	2196	< 0.6	< 20			< 10	6		
$29/2^- \rightarrow 27/2^-$	2214.2	2550	3.3	> 90	0.05(2)	0.045(15) ^b		5	0.09(4)	0.32
$29/2^- \rightarrow 25/2^-$	(1888)	2116	< 0.4	< 10			< 70	58		
$31/2^- \rightarrow 27/2^-$	2691.1	2984	3.0	60(6)	0.10(2)	< 0.12 ^b	35(8)	59		
$31/2^- \rightarrow 29/2^-$	476.3	434	2.0	40(6)	"	"		3	2.1(5)	2.35

Errors in γ -ray energies are 0.4 keV rising to 1 keV above 2 MeV. Gamma-ray lines in brackets were not observed.

^aRef. [22].

^bRef. [12].

^cAlso with NGTB.

^dOnly the partner line was analysed.

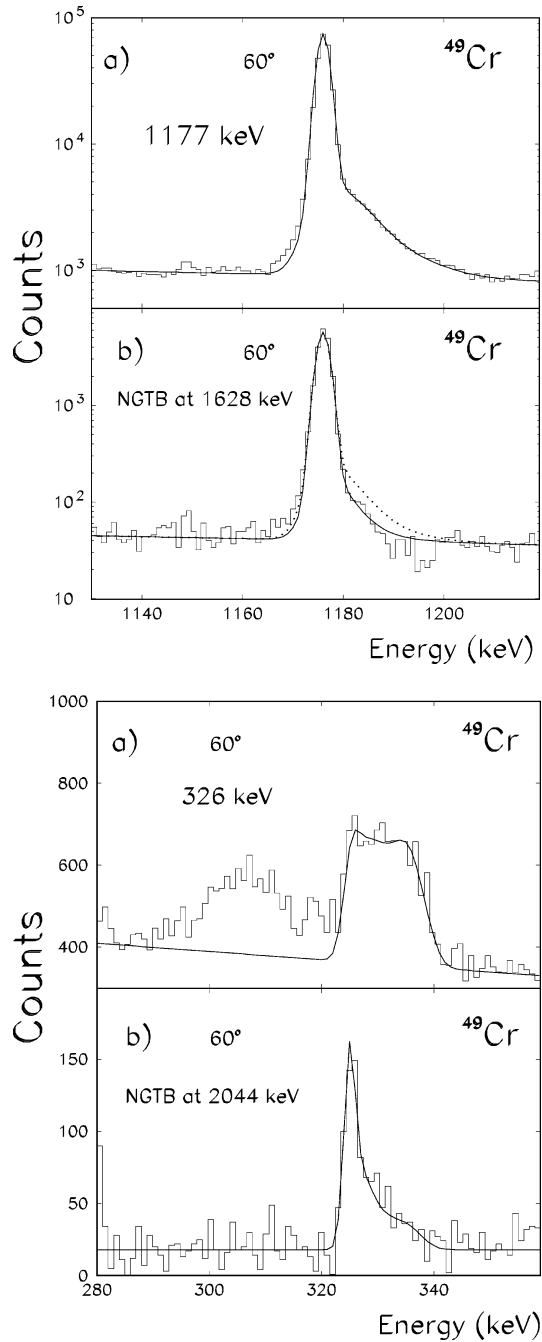


Fig. 5. DSAM lineshape analysis in ^{49}Cr : (upper part) NGTB procedure for the $15/2^-$ state, gating on the 1628 keV $15/2^- \rightarrow 11/2^-$ transition, and using as probe the 1177 keV $19/2^- \rightarrow 15/2^-$ transition; (lower part) NGTB procedure for the $27/2^-$ state, gating on the 2044 keV $27/2^- \rightarrow 23/2^-$ transition, and using as probe the 326 keV $25/2^- \rightarrow 27/2^-$ transition.

of the NGTB analysis of the 1628 keV transition, which leads to a very short lifetime of 0.12(3) ps for the $15/2^-$ state. The dotted curve corresponds to the value of 0.4 ps reported in Ref. [28]. In that case much smaller suppression would occur. The second example shown in the lower part of Fig. 5, refers to the NGTB analysis for the $27/2^-$ state, gating on the 2004 keV line and using the 326 keV $31/2 \rightarrow 27/2^-$ as probe. It is very remarkable that the lifetime obtained in this way fully agrees with the value obtained with a standard analysis, taking into account the feeding transitions. This confirms the placement of the 326 keV transition in the level scheme. The $B(E2)$ and $B(M1)$ values for stretched transitions are in good agreement with LSSM. We note, moreover, that the experimental values of mixing ratios for $\Delta I = 1$ transitions lead to $B(E2)$ rates consistent with theory.

4. Discussion

LSSM calculations were performed with the code ANTOINE [5], using the KB3 residual interaction [29]. Theoretical level schemes were already published for both natural and unnatural parity yrast bands in ^{47}V [9] and for the natural parity band in ^{49}Cr in Ref. [8], to which we refer for details. We only mention that the agreement is in every case within few hundreds of keV.

4.1. The nucleus ^{47}V

The $B(E2)$ rates are generally in good agreement with the theoretical predictions. A deformation parameter $\beta \simeq 0.24$ is deduced for the observed transitions from states with lower spin, under the assumption of a band with $K = 3/2^-$. In a Cranked Shell Model description, however, a triaxial shape with $\gamma \simeq 15^\circ$ is predicted for the neighboring ^{46}V [30]. Triaxiality may explain the very large signature splitting for the natural parity band in ^{47}V and in this case the β parameter would be larger. It must be noted, however, that strong staggering has been obtained by the projected shell model calculations using a deformed basis with axial symmetry [31]. Besides, the analysis made in Ref. [8] in the framework of the quasi- $SU(3)$ model, concludes that ^{48}Cr is axial and so would be ^{47}V .

The $B(E2)$ smooth behavior, predicted at low spin in agreement with the experiment, is suddenly interrupted by a nearly vanishing $B(E2)$ value for the yrast $17/2^-$ state, which has not been observed in this experiment. An experimental observation of this state and the measurement of its properties is a challenge for future experiments.

The experimental $B(M1)$ values clearly confirm the very pronounced staggering predicted by the LSSM calculations. Some M1 transitions, however, could not be observed, as consequence of the large signature splitting. It is remarkable that such staggering is an effect related to a $1f_{7/2}^n$ configuration. In fact, in the empirical $1f_{7/2}^n$ configuration space [12] an even bigger staggering is predicted at low spin, which is, in the actual case, somewhat dumped by configuration mixing.

The positive-parity band has been compared with LSSM in Ref. [9]. Now, the comparison can be done in more detail owing to the better precision of the present data.

The agreement between experimental and theoretical reduced rates is in general good. The quadrupole deformation parameter $\beta \simeq 0.30$, deduced from low-spin transitions, is similar to that of ^{48}Cr [3], thus confirming that the band is due to the coupling of a $d_{3/2}$ proton-hole with ^{48}Cr and hence its shape coexistence with respect to the ground-state band. Only an upper limit could be assigned to the fast higher transitions. Good agreement was achieved for the branches of the $35/2^+$ terminating state, which agree with experimental ones within error bar. On the contrary, disagreement has been found for the decay of the $33/2^+$ state, which is calculated to proceed with comparable intensity via $\Delta I = 1$ and $\Delta I = 2$ transitions, while experimentally the $\Delta I = 2$ branch is not observed. This seems be correlated to the fact that the energy of the $29/2^+$ level is poorly predicted, so that the energy of the $33/2^+ \rightarrow 29/2^+$ transition is calculated to be 475 keV larger than the one experimentally observed. The unobserved M1 transitions are predicted to have a $B(\text{M1})$ value less than $0.03 \mu_N^2$.

4.2. The nucleus ^{49}Cr

In ^{49}Cr , a deformation $\beta \simeq 0.26$ is extracted from lower transitions, under the assumption of $K = 5/2^-$. A small triaxiality could be present in this case according to Ref. [8]. The $19/2^-$ yrast state lies, however, much lower than expected assuming a rotational collective behavior. This can be correlated with the backbending in ^{48}Cr , if we interpret ^{49}Cr as a particle in a deformed orbit coupled to a rotor. As shown in the left part of Fig. 6, the experimental $B(\text{E}2)$ values for the ground-state band agree with theoretical predictions, which show a smooth decrease approaching the band termination

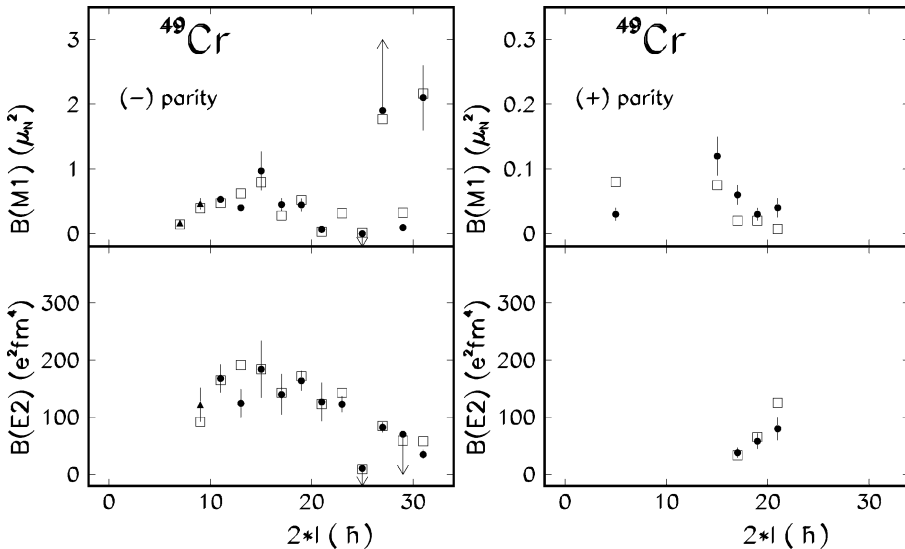


Fig. 6. Experimental $B(\text{E}2)$ and $B(\text{M}1)$ reduced transition rates in ^{49}Cr , compared with LSSM predictions (empty squares). Data are taken from the present work (full circles), except for those indicated as full triangles [22].

with the important exception of the $25/2^-$ level for which the calculated $B(E2)$ value is very small. The observed limit for the $B(E2)$ value of that transition is consistent with LSSM predictions. In this nucleus the staggering of the $B(M1)$ is predicted by LSSM only for the highest transitions, probably because of a large configuration mixing at low spins, possibly related to a larger deformation compared with ^{47}V . Finally, the already published reduced rates of the positive parity bands [4] are shown in the right part of Fig. 6, for reason of completeness.

5. Conclusions

The present study underlines further the great success of SM calculation in the full fp configuration space in explaining the level structure of natural-parity states of nuclei in proximity of ^{48}Cr . The good reproduction of the $B(E2)$ and $B(M1)$ reduced rates for the odd- A nuclei ^{47}V and ^{49}Cr allows the understanding of the interplay between spherical and collective features. In particular, the $B(E2)$ values clearly show the building up of collectivity at low spin in the bands of both natural and nonnatural parities. The collectivity is reduced when approaching the band termination, as the levels become rather pure $1f_{7/2}^n$ states. On the other hand, the $B(M1)$ values show for the natural parity band a big staggering, when approaching the band termination, as they are particularly sensitive to single-particle features. This is a property of spherical $1f_{7/2}^n$ configuration and for the less deformed nucleus ^{47}V is evident also at rather low spin. The sideband in ^{47}V turned out to have a deformation similar as the ground-state band in ^{48}Cr and thus is confirmed the interpretation of a $d_{3/2}$ proton-hole coupled to the ^{48}Cr nucleus [9]. The close comparison with LSSM was possible in virtue of the quality of a multidetector array as GASP and also because of the availability of the new DSAM procedure NGTB [15]. It has to be stressed, however, that some facets remain a challenge for the future: in particular, the observation of the yrast $17/2^-$ state in ^{47}V and the determination of the decay of the $25/2^-$ state in ^{49}Cr . A further goal will be to extend the study to yrare levels, for which interesting structure effects are predicted by theory: so far some transitions have been observed, which could not be placed in the level scheme.

Acknowledgements

R.V.R. and N.H.M. would like to acknowledge financial support from the Brazilian agency CNPq (Conselho Nacional de Desenvolvimento Científico e Tecnológico) and INFN (Italy). A.P. and J.S.S. are supported by a DGES (Spain) grant PB96-53. A.G. was supported by the EC under contract ERBCHBGCT940713. Enlightening discussions with P. Petkov are gratefully acknowledged.

References

- [1] S.M. Lenzi et al., *Z. Phys. A* 354 (1996) 117.
- [2] S.M. Lenzi et al., *Phys. Rev. C* 56 (1997) 1313.
- [3] F. Brandolini et al., *Nucl. Phys. A* 642 (1998) 387.
- [4] F. Brandolini et al., *Phys. Rev. C* 60 (1999) 041305.
- [5] E. Caurier et al., *Phys. Rev. C* 50 (1994) 225.
- [6] E. Caurier et al., *Phys. Rev. Lett.* 75 (1995) 2466.
- [7] G. Martinez-Pinedo et al., *Phys. Rev. C* 54 (1996) R2150.
- [8] G. Martinez-Pinedo et al., *Phys. Rev. C* 55 (1997) 187.
- [9] A. Poves, J. Sanchez-Solano, *Phys. Rev. C* 58 (1998) 179.
- [10] A.P. Zuker et al., *Phys. Rev. C* 52 (1995) R1741.
- [11] J.D. McCullen, B.F. Bayman, L. Zamick, *Phys. Rev.* 134 (1964) 515.
- [12] W. Kutschera, B.A. Brown, K. Ogawa, *Riv. Nuovo Cimento* 1 (1978) 12.
- [13] J.A. Cameron et al., *Phys. Rev. C* 58 (1998) 808.
- [14] F. Brandolini et al., in: *On-line proceedings Selected Topics on $N = Z$ Nuclei*, June 6–10, 2000, Lund, Sweden; <http://pingst2000.kosufy.lu.se>.
- [15] F. Brandolini, R.V. Ribas, *Nucl. Instrum. Methods A* 417 (1998) 150.
- [16] F. Brandolini et al., *Phys. Rev. C* 60 (1999) 024310.
- [17] J.C. Wells, N. Johnson, Report No. ORNL-6689, 1991, p. 44.
- [18] L.C. Northcliffe, R.F. Schilling, *Nucl. Data Tables A* 7 (1970) 233.
- [19] J. Lindhard, M. Scharff, H.E. Schiøtt, *Mat. Fys. Medd. Dan. Vidensk Selsk.* 33 (14) (1963) 7.
- [20] J.F. Ziegler, J.P. Biersack, V. Littmark, in: *The Stopping Power and Range of Ions in Solid*, Vol. 1, Pergamon Press, New York, 1985.
- [21] F. Brandolini et al., *Nucl. Instrum. Methods B* 132 (1997) 11.
- [22] J. Lindhard, M. Scharff, *Phys. Rev.* 124 (1961) 128.
- [23] S.H. Sie et al., *Nucl. Phys. A* 291 (1977) 11.
- [24] L.K. Peker, *Nucl. Data Sheets* 68 (1993) 271.
- [25] M.A. Bentley et al., *Phys. Lett. B* 437 (1998) 243.
- [26] T.W. Burrows, *Nucl. Data Sheets* 74 (1995) 1.
- [27] C.D. O’Leary et al., *Phys. Rev. Lett.* 79 (1997) 4349.
- [28] T.W. Burrows, *Nucl. Data Sheets* 76 (1995) 191.
- [29] A. Poves, A.P. Zuker, *Phys. Rep.* 70 (1981) 235.
- [30] C.D. O’Leary et al., *Phys. Lett B* 459 (1999) 73.
- [31] V. Velasquez, J.G. Hirsch, Yang Sun, *Nucl. Phys. A* 686 (2001) 129.